Organic Metabolite Uptake by Diazotrophs in the North Pacific Ocean

Running title: Organic metabolite uptake by diazotrophs

[1,2,3]Alba Filella, [4]Aurélie Cébron, [5]Benoît Paix, [6,7]Marine Vallet, [1]Pauline Martinot, [1]Léa Guyomarch, [1]Catherine Guigue, [1]Marc Tedetti, [1]Olivier Grosso, [8]Kendra A. Turk-Kubo, [9]Lasse Riemann, [1,2,10,*]Mar Benavides

[1]Aix Marseille Univ, Université de Toulon, CNRS, IRD, MIO UM 110, 13288, Marseille, France

[2]Turing Center for Living Systems, Aix-Marseille University, 13009 Marseille, France

[3]Department of Molecular and Cellular Biology, The University of Arizona, Tucson, AZ, USA

[4]Université de Lorraine, CNRS, LIEC, Nancy, France

[5]UMR CARRTEL, INRAE - Université Savoie Mont-Blanc, Thonon-les-Bains, France

[6]Max Planck Fellow Group Plankton Community Interactions, Max Planck Institute for Chemical Ecology Jena, Germany

[7]Institute for Inorganic and Analytical Chemistry, Friedrich Schiller University of Jena, Jena, Germany

[8]Ocean Sciences Department, University of California, Santa Cruz, Santa Cruz, CA, USA

[9]Department of Biology, University of Copenhagen, Denmark

[10]National Oceanography Centre, European Way, SO14 3ZH Southampton, UK

*Corresponding author: mar.benavides@noc.ac.uk

National Oceanography Centre

European Way, Southampton, SO14 3ZH, UK

Author's contributions

AF and MB designed the experiment and conceived the idea of the manuscript. AF did the incubations and collected the data. AF and CG prepared the phytoplankton-derived DOM. PM, LG and CG analyzed the DOC, CDOM and FDOM samples. MT and PM processed the CDOM and FDOM data. OG ran IRMS and MIMS analyses. MV prepared the samples and performed the data acquisition for metabolomics. MV and BP analyzed and annotated the metabolomics datasets. AC trained AF for DNA-SIP analysis and both processed the samples. AF carried out the formal data analyses, statistics and graphs. AF and MB wrote the manuscript with input from all co-authors.

Abstract

Dinitrogen (N_2) fixation by diazotrophs supports ocean productivity. Diazotrophs include photoautotrophic cyanobacteria, non-cyanobacterial diazotrophs (NCDs) and the recently discovered N_2-fixing haptophyte. While NCDs are ubiquitous in the ocean, their ecology and metabolism remain largely unknown. Unlike cyanobacterial diazotrophs and the haptophyte, NCDs

are primarily heterotrophic and depend on dissolved organic matter (DOM) for carbon and energy. However, conventional DOM amendment incubations do not allow discerning how different diazotrophs use DOM molecules, limiting our knowledge on DOM-diazotroph interactions. To identify diazotrophs using DOM, we amended North Pacific microbial communities with ^{13}C-labeled DOM from phytoplankton cultures that was molecularly characterized, revealing the dominance of nitrogen-rich compounds. After DOM additions, we observed a community shift from cyanobacterial diazotrophs like *Crocosphaera* and *Trichodesmium* to NCDs at stations where the N_2-fixing haptophyte abundance was relatively low. Through DNA stable isotope probing and gene sequencing, we identified diverse diazotrophs capable of taking up DOM. Our findings highlight unexpected DOM uptake by the haptophyte's nitroplast, changes in community structure, and previously unrecognized osmotrophic behavior in NCDs, shaped by local biogeochemical conditions.

Keywords: DNA-SIP, *nifH*, osmotrophy, N_2 fixation, DOM, DOM composition, mixotrophy, NCDs

Introduction

Marine microorganisms called diazotrophs fix dinitrogen (N_2) into ammonium, providing a critical source of reactive nitrogen in marine ecosystems. Research has traditionally focused on cyanobacterial diazotroph species such as the filamentous *Trichodesmium*, the unicellular *Crocosphaera* and UCYN-A (e.g., 1–3), recently reconsidered as an early-stage organelle (the 'nitroplast') of the haptophyte *Braarudosphaera bigelowii* [4]. However, non-cyanobacterial diazotrophs (NCDs) have a broader distribution than cyanobacterial diazotrophs in marine ecosystems, often representing the largest proportion of the community based on nitrogenase gene (*nifH*) amplicon sequencing [5, 6]. Still, the contribution of NCDs to N_2 fixation inputs remains poorly constrained [7].

Contrary to cyanobacterial diazotrophs and the N_2-fixing *B. bigelowii* that obtain carbon and energy from photosynthesis, metagenome-assembled genomes (MAGs) indicate that NCDs have the genetic machinery to obtain carbon, nutrients and energy from organic matter through a wide range of metabolic strategies, including photo- and chemoheterotrophy [8–11]. Several studies have reported enhanced bulk N_2 fixation rates, *nifH* gene expression, and growth of NCDs in response to dissolved organic matter (DOM) additions, including proteobacteria and Cluster-III taxa [12–14]. However, cyanobacterial diazotrophs also respond to DOM additions with enhanced growth rates and *nifH* gene expression (e.g., 13, 15–19), suggesting that DOM affects N_2 fixation inputs by both cyanobacterial and NCDs.

By controlling nitrogen availability in vast ocean regions, diazotrophs sustain marine productivity and contribute to carbon sequestration and the regulation of climate [20]. In turn, climate change-induced stresses on diazotrophs, such as decreased activity under high temperatures and low pH, can be alleviated by DOM uptake [21]. Investigating DOM-diazotroph interactions is needed to

improve our understanding of their current and future role as key nitrogen suppliers. This can be a daunting task due to the high molecular complexity of DOM [22]. Our current understanding of DOM-diazotroph interactions is based on incubation experiments where field or cultured diazotrophs are incubated with relatively simple DOM molecules such as glucose or mannitol, which do not reflect the complexity of the marine DOM pool [22–24]. Marine DOM is mainly produced by phytoplankton photosynthates, subsequently consumed and transformed by heterotrophs and altered by abiotic factors such as solar radiation [25–27]. As a result, labile DOM only represents 0.03% of the total dissolved organic carbon contained in marine DOM (662.2 Pg C; 28). The chemical composition of DOM is not fully known. However, techniques such as ultra-high resolution mass spectrometry have identified > 20,000 molecular formulas with > 30 isomers each, totaling > 600,000 compounds, although marine DOM may contain several million distinct organic compounds [28–30].

Given the wide diversity of both diazotroph species and DOM compounds, establishing links between them has proven challenging (e.g., 14, 16). Indirect approaches such as measuring bulk N_2 fixation rates in response to DOM additions integrate the signals from the entire diazotroph community and cannot resolve which diazotroph taxa are actively consuming DOM compounds. DNA Stable-Isotope Probing (DNA-SIP) offers a means of tracing isotopically labeled substrates into DNA, allowing microbial identity to be linked to catabolic activity [31]. Here, we investigate the uptake of phytoplankton-derived DOM by diazotroph communities in the North Pacific Ocean. Using DNA-SIP with a molecularly characterized DOM substrate, we provide direct evidence of DOM uptake by different diazotrophic taxa. Our results suggest that DOM plays an essential role for photoautotrophic and chemoorganoheterotrophic diazotrophs alike, revealing novel osmotrophic metabolisms and ecological strategies allowing them to thrive under unfavorable conditions and expand their traditional niche.

Materials and Methods

Experimental design and sampling procedure

This study was conducted during the NCD cruise (KM2206) between 4th June and 6th July 2022 onboard the R/V *Kilo Moana*. The cruise took place in the North Pacific Subtropical Gyre, west of the Hawaiian Islands between 15-30ºN and 159-179ºW (Fig. 1A). Seawater was collected from four stations (2, 4, 11 and 26; Fig. 1A) at 15 m depth and distributed into individual 4.5 l polycarbonate bottles (Nalgene, Rochester, NY, USA) to measure background conditions (time zero or 'T0'), DOM uptake, and N_2 fixation rates, and perform DNA-SIP analyses (Fig. 1B; Supplementary Information). Phytoplankton-derived DOM was extracted from cultures of *Synechococcus* sp. RCC2033 and *Thalassiosira pseudonana* previously grown in the lab following Kieft et al., [23]; see Supplementary Information for more details on $^{13}C/^{12}C$-labeled DOM production). This phytoplankton-derived DOM was added to the 'DOM incubation bottles' to a final concentration of 8 µM C (~10% of background dissolved organic carbon (DOC) in surface waters of the North Pacific; 32, 33) (Fig. 1). All incubations were performed on-deck incubators with flowing surface seawater for 24 h at *in situ* temperature in the dark (to reduce any osmotrophic signal from diazotrophic cyanobacteria and focus on that of NCDs). Subsamples for DOC, chromophoric and fluorescent DOM (CDOM and FDOM, respectively), dissolved inorganic nutrients (phosphate and nitrate, see below), and heterotrophic bacteria abundance were collected from all experimental bottles at the beginning of the experiment (T0), and after 18 h (T18) and 24 h (T24) of incubation (Fig. 1B; Supplementary Information). The volume remaining after sampling for DOC, CDOM, and FDOM was filtered either for DNA extractions (4 l onto 0.2 µm polysulfone membrane filters; Supor, Pall, Ann Arbor, MI, USA) or for particulate organic matter (POM; 4.4 l onto combusted GF/F filters; Whatman, Maidstone, UK) and POM isotopic enrichments analyses to measure N_2 fixation and DOM uptake rates (see below; Supplementary Information).

Water column measurements, nutrient and DOM analyses

A conductivity, temperature, and depth probe (CTD 9/11plus, Sea-Bird Scientific) mounted on a 24-Niskin bottle rosette sampler was used to measure hydrographic properties in the water column. Additional sensors included turbidity, beam attenuation, and Chlorophyll-a fluorescence. Samples for the measurement of nitrate and phosphate concentrations were obtained after filtration through GF/F filters in 20 ml Teflon vials and stored at -20°C until analysis (Supplementary Information). Samples for DOC, CDOM, and FDOM were collected by filtering through Milli-Q water- and sample-rinsed 0.45 µm GMF GD/X syringe filters (Whatman, Florham Park, New Jersey, USA) and stored in combusted (500°C, 4 h) 20 ml glass vials in the dark at 4 °C prior to analysis (Supporting Information).

Molecular characterization of phytoplankton-derived DOM

Liquid chromatography coupled with high-resolution mass spectrometry was used simultaneously to detect and identify the metabolites in the phytoplankton-derived DOM extracts produced in the lab for onboard *in situ* incubations (see Supplementary Information). To analyze the (i) polar and (ii) apolar low-weight compounds, we injected 1 µl of each ^{13}C-DOM and ^{12}C-DOM extracts in triplicates and run them through a ZIC-HILIC column (150 x 2.1 mm, 5 µm) and a Silica C18 column (100 x 2.1 mm, 2.6 µm), respectively (see Supplementary Information for more details). The identity of selected compounds was confirmed with tandem mass spectrometry, and the MS/MS spectra were compared by spectral similarity search in Global natural product social networking (GNPS; see Supplementary Information).

The two data matrices were analyzed using the MetaboAnalyst 5.0 web tool [34], resulting in tables with ^{12}C and ^{13}C isotopic peaks from the same compounds as distinct variables (separated rows). Quantile normalization and normalization by sum methods were applied to the C18 and ZIC-HILIC datasets, respectively. Volcano plots were generated to identify the significant features discriminating between labeled and unlabeled DOM samples, using a fold change (FC) threshold of 2 and a *p* value threshold of 0.05 with False Discovery Rate correction.

DNA-SIP

DNA-SIP experiments were performed by incubating natural planktonic communities with either heavily labeled (^{13}C) or unlabeled (^{12}C) DOM we had previously prepared from phytoplankton cultures in the lab [31, 35, 36] (Supplementary Information). The rationale behind using both heavy (^{13}C) and light (^{12}C) isotopes of the substrate of interest (here carbon contained in the DOM mixture) is to allow separation of the DNA of the substrate-incorporators by density differences (Supporting Information). After DNA extractions (see Supporting Information), heavy (high ^{13}C-labelling) DNA was separated from light (low ^{13}C-labelling and high ^{12}C-labelling) DNA using a density gradient for both treatments, separating different molecular weight DNA fractions according to Neufeld et al. [31] (Supplementary Information). To verify the success of the DNA-SIP steps and determine the distribution of the DNA fractions after isopycnic separation, the abundance of 16S rRNA genes in each density fraction was quantified by quantitative PCR (qPCR). The qPCR assay was performed using the primers 968F and 1401R [37] as described in Cébron et al. [38] (Supporting Information). Based on the distribution of DNA and 16S rRNA copies along the density gradient and the comparison of ^{13}C-enriched and ^{12}C-enriched DNA samples (Fig. S1), we selected four consecutive DNA fractions here called heavy or 'H', medium or 'M', light or 'L' and super-light or 'SL' for downstream sequencing analyses (*nifH* and 16S rRNA gene amplicon sequencing; see Supplementary Information).

Statistical analyses

The integrated development environment for the statistical software R, RStudio (RRID: SCR_000432, Version 2023.12.1+402), was used to process and analyze the data and to generate graphs. All differences between treatments or stations for all parameters and other statistical patterns were evaluated by one-way ANOVA, after checking data for normality and heterogeneity of variance (QQ plot, Shapiro–Wilk test, and Levene's test). Significant differences in the relative abundance of *nifH* or 16S rRNA genes between the two treatments (^{13}C vs. ^{12}C) were tested using the Wilcoxon test. Statistical significance for all tests was set at a *p*-values less than 0.05 (95% confidence level).

Results

Biogeochemical and environmental patterns

Sea surface (< 15 m) temperature and salinity differed significantly among stations (ANOVA, $p < 0.0001$; Fig. S2A-B), being highest at stations 26 and 11 (28 °C and 35.3, respectively), and lowest at stations 4 and 2 (24 °C and 34.9, respectively). Fluorescence and beam attenuation at the same depth were higher at stations 2 and 4 than at stations 11 and 26 (ANOVA, $p < 0.0001$; Fig. S2B, D; Supplementary Information). Nitrate and phosphate concentrations at 15 m ranged from 0.003 to 0.061 µM and from 0.007 to 0.060 µM, respectively, with the highest average concentrations observed at stations 26 and 2 and the lowest at station 4 (Fig. S2E-F). DOC concentrations at the same depth were lower at stations 2 and 4 (70 µM) than at the other two stations (84 µM) (ANOVA; $p < 0.001$; Fig. S2G). The CDOM absorption coefficient at 325 nm (a_{325}) and the humification and biological FDOM indices (HIX and BIX, respectively), indicated that DOM at station 2 (highest BIX, lowest a_{325}) was fresher/more aliphatic than elsewhere. In contrast, DOM at station 4 (highest HIX,

low BIX, high a_{325}) displayed a more humic/aromatic character (Fig. S2I-K; 39, 40). The average molecular weight of bulk DOM, depicted by the CDOM absorption spectral slope between 275 and 295 nm ($S_{275-295}$), was higher at station 2 (lowest $S_{275-295}$ values) and lower at the other stations (Fig. S2L). The high values of $S_{275-295}$ and a_{325} at stations 4, 11, and 26 (Fig. S2K, L) indicated the dominance of low molecular weight and aromatic compounds, which potentially underwent photobleaching or other degradation processes [41].

Molecular composition of phytoplankton-derived DOM

Two data matrices were obtained for metabolite analyses of the phytoplankton-derived DOM extracts (^{12}C and ^{13}C) produced in the lab (Supplementary Information) and used as substrate in our onboard experiments. Together with the investigations of the isotopic peaks (Tables S1, S2), volcano plots using both datasets indicated that most ^{13}C isotopic peaks were more abundant in the ^{13}C-DOM extract (right side), whereas the ^{12}C isotopic peaks were more abundant in the ^{12}C-DOM (left side) (Fig. S3). Moreover several compounds, for example methyl-guanosine and valeryl-carnitine, showed high ^{13}C atom enrichment (Fig. S4). Thus, these analyses confirmed that the composition of ^{12}C- and ^{13}C-DOM was very similar (Supporting Information), which is a prerequisite for DNA-SIP analysis [31]. After metabolite annotation, both datasets showed that the prominent chemical families corresponded to nitrogen-containing molecules such as amino acids (e.g., arginine, tryptophan), dipeptides (e.g., alanyl-leucine, glycyl-leucine), nucleosides (e.g., deoxyadenosine, deoxyguanosine), and carnitine derivatives (e.g. acetylcarnitine, propionylcarnitine) (Tables S1, S2). In addition, zwitterions such as dimethylsulfoniopropionate (DMSP) and choline were identified (Tables S1, S2).

Impact of phytoplankton-derived DOM on N_2 fixation

Background (T0) concentrations of particulate organic carbon (POC) and nitrogen (PON) (i.e., before DOM additions) were highest at stations 26 and 2, respectively (Fig. 2). POC and PON concentrations in the control incubations did not change after 24 h and were not significantly different from T0 values (*t*-test; $p > 0.1$; Fig. 2). Instead, a significant increase in both POC and PON was observed at all stations following DOM additions (*t*-test; $p < 0.01$; Fig. 2), with the highest and lowest POC and PON build-up measured at stations 2 and 11, respectively (Fig. 2A).

Given the potential inflation of bulk N_2 fixation rates by background PON concentrations [42, 43], in this study we report the fractional ^{15}N-enrichment of the particulate nitrogen (^{15}N at %) which provides a more accurate measure of diazotrophic activity (N_2 fixation). The ^{15}N at% enrichment of bulk PON was higher in controls than in DOM-amended incubations at all stations (*t*-test, $p < 0.05$; Fig. 2B). Still, the ^{15}N at% PON in DOM-amended samples was significantly higher than in T0 samples at all stations, except at station 2 (*t*-test, $p > 0.1$; Fig. 2B). The highest ^{15}N at% PON values were observed at stations 26 and 11, which showed similar values (*t*-test, $p > 0.05$; Fig. 2B) regardless of whether the samples were DOM-amended or not (Fig. 2B). All DOM-amended samples showed significantly higher ^{13}C at% POC enrichment than control and T0 samples (*t*-test, $p < 0.05$; Fig. 2B). The highest ^{13}C at% POC was measured at station 4 and the lowest in one of the replicates at station 2, while all replicates at station 26 consistently showed the lowest values (Fig. 2B).

Diazotroph community (nifH genes) response to DOM additions

Phytoplankton-derived DOM additions caused a shift from diazotrophic cyanobacteria to NCDs (*nifH* genes) at stations where the abundance of the N_2-fixing haptophyte was lower (stations 11 and 26). The T0 diazotroph community composition was heavily dominated by cyanobacteria over NCDs (93.1% over 6.9% of *nifH* reads) at all stations (Fig. 3A). Stations 2 and 4 showed the highest relative abundance of the *B. bigelowii* nitroplast (86.8% and 97%, respectively; Fig. 3B), previously referred

to as UCYN-A. The relative abundance of the nitroplast at station 11 was similar to that of *Crocosphaera* (35.7% and 41.1% of *nifH* reads, respectively). In contrast, *Crocosphaera* dominated at station 26 (99.6%; Fig. 3B). *Trichodesmium nifH* reads were found at low relative abundance at stations 2 and 26 (6.5% and 0.1%, respectively; Fig. 3B). The few NCDs at T0 were mainly assigned to the Alcaligenaceae family (betaproteobacteria)(Fig. 3A), particularly at station 11 (Fig. 3B).

After 24 h of incubation, the relative abundance of the nitroplast in control incubations decreased by 35.6% and 12.5% at stations 2 and 11, respectively, but remained almost constant at station 4 (Fig. 3B). The initially high relative abundance of *Crocosphaera* at station 26 remained relatively constant during the incubation but increased to 36.1% and 7.0% at stations 2 and 11, respectively (Fig. 3B). The relative abundance of *Trichodesmium* at station 2 also decreased during the control incubations (Fig. 3B). Conversely, an alphaproteobacterium of the genus *Marinibacterium* had higher relative abundance (20.5% and 1.0% at station 11 and 26, respectively) in control incubations than at T0 (Fig. 3B).

Phytoplankton-derived DOM additions increased the relative abundance of two alpha- and one gammaproteobacteria NCDs annotated as *Sagittula*, *Marinibacterium* and *Marinobacterium,* respectively, at stations 26 and 11 (Fig. 3B). The relative abundance of the nitroplast in DOM-amended incubations decreased by 17.5 and 14.3% at stations 4 and 11, respectively, and only slightly (2.5%) at station 2. No *Trichodesmium nifH* reads were detected in the DOM-amended samples, and *Crocosphaera* was only detected at low abundance at stations 11 and 26 (0.4% and 0.1% of total *nifH* reads, respectively) (Fig. 3).

Beyond bulk changes in the relative abundance of the *nifH* gene between control or DOM-amended incubations (Fig. 3), DNA-SIP analyses allowed us to identify which diazotrophic taxa incorporated organic carbon from the added DOM mixture (Fig. 4). We examined changes in the relative

abundance of *nifH* genes in the H, M, L and SL DNA density fractions comparing ^{13}C- and ^{12}C-DOM amended samples (Fig. 4). The nitroplast (Fig. 4A), the alphaproteobacteria *Sagittula* and *Marinibacterium* (Fig. 4B-C), and the gammaproteobacterium *Marinobacterium* (Fig. 4D) were the main diazotrophs showing evidence of DOM incorporation (Fig. 4). The relative abundance of the nitroplast was higher in the H ^{13}C DNA fraction than in the H ^{12}C DNA fraction at stations 2 and 4 (Kruskal-Wallis test; $p < 0.0001$; Fig. 4). The *nifH* genes of the alphaproteobacteria *Marinibacterium* and *Sagittula* were not detected in H ^{12}C DNA fractions, while their relative abundance represented 11.8% and 35.2% of the *nifH* relative abundance in the H ^{13}C DNA fraction (Fig. 4B-C). The relative abundance of the gammaproteobacterium *Marinobacterium* was slightly higher in the H ^{13}C DNA fraction than in the H ^{12}C DNA fraction (Kruskal-Wallis test; $p = 0.6102$; Fig. 4D). Moreover, the *nifH* relative abundance of the nitroplast, *Marinibacterium* and *Marinobacterium* in M ^{13}C DNA fractions were also 1.32, 3.59 and 1.31 times higher than in M ^{12}C DNA fractions treatment at stations 4, 11 and 26, respectively (Kruskal-Wallis test; $p < 0.01$; Fig. 4).

Overall prokaryote community (16S rRNA genes) response to DOM additions

16S rRNA gene amplicon sequencing revealed that phytoplankton-derived DOM additions significantly increased the relative abundance of several alpha- and gammaproteobacteria groups, while alphaproteobacteria showed higher osmotrophic capacities. Groups of alphaproteobacteria dominated at T0 at all stations (29.8-44.3%), followed by the non-diazotrophic cyanobacterium *Prochlorococcus* (21.1-30.2%) (Fig. 5A). Gammaproteobacteria and Bacteroidia represented 13.2-15% and 9.7-13.2% of the total prokaryotic community, respectively, showing less variability among stations (Fig. 5A). In general, the abundance of heterotrophic bacteria estimated by flow cytometry (cells ml^{-1}) did not vary during control incubations (*t*-test; $p > 0.1$; Fig. S5A), except at station 2 where their abundance increased significantly over the incubation period (*t*-test; $p = 2 \times 10^{-5}$). In control incubations, the initially dominant alphaproteobacteria belonging to SAR11 clades Ia and Ib, and the

marine group AEGEAN-169 were present together with *Prochlorococcus,* but their relative abundance did not change by more than 6% as compared to T0 (Fig. 5B).

The abundance (cells ml^{-1}) of heterotrophic bacteria increased at all stations following DOM additions ($p < 0.1$; Fig. S5B), being mostly representatives of alpha- and gammaproteobacteria groups (Fig. 5B). However, most groups showed similar relative abundances between ^{13}C- and ^{12}C-DOM incubations when contrasting different DNA density fractions (e.g., H or M; Fig. 6), suggesting no DOC incorporation. This was the case for most gammaproteobacteria, including *Pseudoalteromonas* and *Alteromonas* (Fig. 5B). Similarly, the relative abundance of some alphaproteobacteria such as *Shimia,* which increased significantly after DOM additions (Fig. 5B), was not higher in the H ^{13}C DNA than in the H ^{12}C DNA fractions (Fig. 6). In contrast, we observed a significant increase in the relative abundance of the alphaproteobacteria *Leisingera* (stations 2 and 11), *Nautella* (stations 11 and 26), *Pseudooceaonicola* (stations 11 and 26) and of *Ruegeria* (stations 2 and 11) in the heavier (H and M) ^{13}C DNA fractions as compared to the corresponding ^{12}C DNA fractions (Fig. 6).

To evaluate the competition and partitioning of DOM between diazotrophic and non-diazotrophic bacteria, we did a co-occurrence network analysis (see Supplementary Information; Fig. S6) using both the *nifH* and 16S rRNA gene reads from the different DNA SIP fractions. These networks showed positive connections between alphaproteobacteria (diazotrophic or not), while negative connections were observed between gamma- and alphaproteobacteria, and between diazotrophic and non-diazotrophic gammaproteobacteria (Fig. S6). Negative relationships between alphaproteobacteria taxa were only observed between T0 abundant oligotrophic groups such as Clade Ia and all alphaproteobacteria taxa after DOM addition, and between *Leisingera* and *Ruegeria* with the nitroplast (Fig. S6).

Discussion

Phytoplankton-derived DOM additions to surface diazotroph communities revealed that both the *B. bigelowii* nitroplast and diverse NCDs were able to take up DOM. However, the response of diazotrophs to DOM additions varied largely among groups and between stations, influenced by temperature, nutrient concentrations, DOM composition and differences in the *in situ* community structure (Fig. S6).

DOM uptake by NCDs

The alphaproteobacteria *Sagittula* and *Marinibacterium*, and the gammaproteobacterium *Marinobacterium* (see Supplementary Information for *nifH* sequence homology) assimilated phytoplankton-derived DOM at the westernmost and warm waters (26.31-27.82 °C; Fig. S2) stations 11 and 26 (Fig. 4). Previous studies have reported gammaproteobacteria as the dominant NCD group in open waters of the Pacific and Atlantic Oceans [5, 44, 45], with their *nifH* gene counts or relative abundances positively correlating with nutrients and DOM availability or primary productivity [13, 14, 46, 47]. In contrast, *nifH* reads of the alphaproteobacterium *Sagittula* negatively correlate with nitrate and phosphate concentrations in regions such as the Eastern Indian Ocean [48]. Consistent with this, the detection of *Sagittula nifH* gene reads at station 11 coincided with low phosphate concentrations (Fig. S2F). Indeed, the genome of *Sagittula* shows diverse metabolic pathways to obtain dissolved organic phosphorus, including phosphonates and phosphoanhydrides [49], which may allow this genus to thrive in phosphate-poor waters when other resources such as DOM are not limiting. While *Sagittula* has been suggested as an important N_2 fixer worldwide (e.g., 49, 50), *Marinibacterium* and *Marinobacterium* have rarely been reported from open ocean samples [51, 52]. *Marinibacterium* MAGs suggest that their metabolism is versatile, including the ability for photoheterotrophy (anoxygenic photosystem II; 52) or to use methanol as a carbon and energy

source (methanol dehydrogenase, *XoxF*; 51). However, our knowledge of their activity and involvement in biogeochemical cycles is still limited.

Based on available reference genomes, both *Sagittula* and *Marinobacterium* are flexible in substrate utilization (e.g., sugars, amino acids, and peptides) and energy acquisition mechanisms, including the degradation of aromatic hydrocarbon compounds [49, 53]. The ^{13}C-DOM substrate used in our incubations contained several compounds (i.e., amino acids and nucleosides; Tables S1, S2) that can be utilized by both *Sagittula* and *Marinobacterium*. For example, *Marinobacterium* can synthesize glycine betaine from choline [53]. Glycine betaine is an important osmoprotectant, as well as dimethylsulfoniopropionate (DMSP) and carnitine, which were present in our DOM mixture (Tables S1, S2). These ubiquitous metabolites and their derivatives, such as DMS, are well known to serve as energy and/or nutrient sources for most prokaryotes [54, 55], including *Sagittula* [49] and even eukaryotes such as marine diatoms [56, 57]. *Sagittula* and *Marinobacterium* may have benefitted similarly from these widespread marine metabolites during our study. Still, *Sagittula* genes encode for the uptake of a wider variety of substrates than *Marinobacterium* species, such as lipopolysaccharides, lipoproteins, tungstate, and thiamine [49], which might explain their prevalence at station 11 where the lowest biomass was observed (Fig. 2). In contrast, *Marinobacterium* is less metabolically versatile but still had higher relative abundances than *Crocosphaera* upon phytoplankton-derived DOM additions at station 26, suggesting an efficient uptake of the added DOM allowing for rapid growth (Fig. 3). This contrasts with previous studies showing DOM uptake by *Crocosphaera* [13, 21]. However, in those studies, photosynthesis was not limited (day/night cycle incubations, while our incubations were 24 h in the dark), and the amended DOM consisted mainly of carbohydrates which were not detected in our ^{13}C-DOM mixture (Tables S1, S2). In addition, the growth rates of different microorganisms may affect the amount of ^{13}C incorporated into DNA at a given time, as DNA needs to be replicated to be detected as a ^{13}C-DOM signal. Therefore, even if slow-growing microorganisms take up significant amounts of ^{13}C-DOM, the incorporation of isotopic

labels in their DNA can be low, while a longer incubation to counteract this problem might introduce bias as cross-feeding events [58].

Overall, our results indicate that different NCD groups grew on DON-rich DOM (Tables S1, S2), allowing them to outcompete other diazotrophs but did not favor bulk N_2 fixation. NCDs are considered facultative N_2 fixers as they show broad flexibility in their nitrogen metabolism [59]. Yet, N_2 fixation rates were detectable after DOM additions and ^{15}N at% PON values were significantly higher than at T0 at stations where *Sagittula*, *Marinibacterium,* and *Marinobacterium* were present (Fig. 2B). These NCDs groups were virtually absent at T0 at stations 11 and 26 but increased their relative abundance upon the addition of phytoplankton-derived DOM. This observation could be due to the low lability of the background DOM at T0 (Fig. S2I-L) or to the dominance of better-adapted photoautotrophic species such as *Crocosphaera.* Our results suggest that *Sagittula*, *Marinobacterium,* and *Marinobacterium* can contribute to DOM uptake and compete with other prokaryotes even when nitrogen metabolites are available.

DOM uptake in the N_2-fixing haptophyte nitroplast

The *B. bigelowii* nitroplast assimilated DOM at the eastern and cooler waters (24.28-25.94 °C; Fig. S2) stations 2 and 4 (Fig. 3; Fig. 4). These stations differed significantly from each other in the background chemical composition and DOM lability (Fig. S2). At station 2, DOM was fresher and had a higher molecular weight (higher BIX and lower $S_{275\text{-}295}$ values characteristic of newly released DOM by either bloom crash or zooplankton grazing 60, 61; Fig. S2J, L) than at station 4, which was more chemically complex and refractory (e.g., higher HIX, a_{325} and $S_{275\text{-}295}$ values; Fig. S2I, K, L). Furthermore, nitrate and phosphate concentrations were the lowest at station 4 (Fig. S2). These differences in the background availability of DOM and nutrients partly explain why higher ^{13}C-DOM assimilation was observed at station 4 than at station 2 (Fig. 4). This indicates that DOM uptake is a

beneficial trait for the coccolithophore *B. bigelowii* under dark and low nutrient availability conditions. At station 2, *B. bigelowii* might have assimilated less DOM or even used some of the more labile background DOM present in ambient waters, resulting in lower incorporation of ^{13}C-DOM and an isotopic dilution of the ^{13}C signal in DNA extracts. Still, ^{13}C-DOM additions at station 2 induced a 15.45-fold increase in the relative abundance (bulk DNA) of nitroplast *nifH* reads (*t*-test; p = 0.075; Fig. 3), suggesting that compounds other than organic carbon in the DOM mixture (e.g., nitrogen-rich amino acids or nucleosides; Tables S1, S2) may have stimulated their growth.

Mills et al. [62] found that *B. bigelowii* does not take up nitrate and assimilates only small amounts of ammonium, suggesting that its nitrogen requirements are met mainly by N_2 fixation by the nitroplast (62; Fig. 7A). However, the nitroplast may fail to meet the nitrogen demand of *B. bigelowii* under conditions where the ratio of carbon fixation/nitrogen transfer or *B. bigelowii*/nitroplast size is unbalanced [62, 63]. In these cases, the *B. bigelowii*/nitroplast is likely to rely on other reactive nitrogen sources such as dissolved organic nitrogen (DON) or bacterial phagotrophy [64]. The nitroplast lacks the genetic machinery to produce some key organic nitrogen compounds, such as amino acids and nucleotides. Still, the nitroplast can incorporate such compounds from the algae via specific amino acid or purine transporters [65] (Fig. 7B). This suggest a intricate exchange of nitrogenous metabolites, with N_2 being fixed into ammonia in the nitroplast and then transferred to *B. bigelowii* [3]. In return, the host metabolizes ammonium into organic nitrogen, which is then transferred to the nitroplast (Fig. 7B).

N_2 fixation (presented as ^{15}N at% enrichment) was undetectable or lower than controls after DOM additions at stations 2 and 4 (Fig. 2), suggesting that DOM inhibited N_2 fixation. Using DOM as a nitrogen source instead of relying on its nitroplast may reduce the overall energy requirements of *B. bigelowii* (Fig. 7C). Flexibility in substrate use and resource allocation may be a key trait of *B. bigelowii*, explaining its ability to thrive from tropical to polar oceans [66, 67], and to survive in

turbid upwelling waters where diazotrophic cyanobacteria are uncompetitive [9, 68]. Indeed, although light appears to be a critical factor controlling the metabolism of the *B. bigelowii* symbiosis, the carbon fixed by the algae might be crucial in regulating N_2 fixation in the nitroplast [69]. The dark incubations used in our experiments may have triggered an osmotrophic response of *B. bigelowii* and subsequent transfer of ^{13}C-DOM to the nitroplast (Fig. 7C) at stations where it was initially abundant. These results call for a review of the role of the *B. bigelowii*/nitroplast ocean DOM cycling in the ocean.

Competition between diazotrophic and non-diazotrophic bacteria for DOM

Bulk POC and PON concentrations increased after DOM additions to dark incubations (Fig. 2), suggesting that microbial growth was DOM-limited without light. The POC ^{13}C at% enrichment confirmed substrate incorporation by the bulk planktonic community at all stations, while the PON ^{15}N at% enrichment was consistently higher in control than in DOM-amended incubations (Fig. 2). This indicates a potential suppression of N_2 fixation by DOM, e.g., by DON metabolites, which constituted most of the molecules detected in our DOM mixture (Tables S1, S2), or the faster uptake of DOM by microbes other than diazotrophs, limiting resources for N_2 fixation (Fig. 5). A combination of these scenarios is likely, and therefore the increase of ^{13}C at% enrichment in bulk POC arguably includes the signal from both diazotrophic and non-diazotrophic microbes (Fig. 2, Fig. 5).

To further understand the competition and partitioning of DOM between diazotrophic and non-diazotrophic bacteria, we evaluated the differences in 16S rRNA gene reads in the different DNA fractions as we did for the *nifH* genes (Fig. 5; Fig. 6). Although the non-diazotrophic prokaryotic community was similar between stations at T0 (Fig. 5A), and in contrast to the diazotrophic community (Fig. 3A), we did not observe an analogous prokaryote response to DOM additions at the different stations (Fig. 5B). Therefore, factors other than the metabolic capabilities of the non-

diazotrophic prokaryotes such as nutrient availability or competition with other planktonic groups may have shaped the DOM uptake at the different stations. In general, the relative abundance of non-diazotrophic prokaryotes increased significantly after DOM additions, especially alphaproteobacteria (Fig. 5B; Fig. S6). Notwithstanding, only a few groups showed ^{13}C-DOM assimilation and their response varied spatially, indicating different use of the DOM and intraspecies competition at the different stations (Fig. 5B; Fig. 6; Fig. S6). For example, the alphaproteobacteria *Leisingera* and *Nautella* increased their relative abundance after DOM addition at most stations, including station 4. Still, they only showed evidence of DOM uptake at stations 2 and 11, and 11 and 26, respectively (Fig. 6). At station 4, where the background DOM was refractory and nutrients were scarce (Fig. S2), DOM additions induced a high ^{13}C at% enrichment of POC (Fig. 2B), suggesting that the *B. bigelowii* nitroplast may be a significant contributor to DOM assimilation at this station. Conversely, the other prokaryotes that increased in relative abundances after DOM addition (bulk DNA) at station 4 may have used the phytoplankton-derived DOM as a source other than organic carbon such as nutrients (e.g., nitrogen-containing metabolites; Tables S1, S2). This could explain the uncoupling between increasing bacterial growth and DOM incorporation, especially at stations 4 and 26 (Fig. 2A; Fig. 5; Fig. S5A). At station 26, the increase in relative abundance of the non-diazotrophic alphaproteobacterium *Ruegeria* and of the two gammaproteobacteria, *Alteromonas* and *Pseudoalteromonas*, in response to DOM additions was also uncoupled from DOM uptake (Fig. 6). Again, these species could have benefited from DOM additions for different purposes such as deriving their sulfur requirements from DMSP, as observed in several *Ruegeria* species [70]. In contrast, another study conducted during our cruise analyzing particle-associated NCDs found that gammaproteobacteria were the most abundant groups [71], suggesting that POM is a more suitable carbon source for gammaproteobacteria NCDs than DOM.

Our results suggest that the variability in ambient nutrients, DOM, and community structure between stations drives contrasting responses to DOM additions between alpha- and

gammaproteobacteria. The negative relationship between these two classes following DOM additions is supported by co-occurrence network analyses (Fig. S6). Moreover, this analysis showed mostly positive connections between alphaproteobacteria taxa (diazotrophic or not), revealing very different ecologies within this class and a diverse and shared exploitaiton of DOM enabling different planktonic groups to benefit from the same substrate. The weak negative relationship between *Leisingera* and the nitroplast at stations 2 and 4 (Fig. S6) indicates some competition between the two groups for the added substrate. Longer incubations and nutrient addition experiments will help disentangle the competition of different bacterial groups for DOM. Such studies emerge as a priority in the increasingly warmer and nutrient-starved subtropical gyres, where competition for DOM substrates between microbial species may influence carbon cycling and contribution of DOM to the biological carbon pump.

Acknowledgements

We would like to thank the captain, crew of R/V *Kilo Moana* and T. Rohrer for field logistical support, and the Ocean Technology Group from the University of Hawai'i for their technical assistance before and during cruise. We thank M. Mills for the help setting up the onboard incubators and pump system during the cruise. The platform of cytometry for microbiology (precym.mio.osupytheas.fr) and S. Nunige are acknowledged for flow cytometry and nutrient analyses, respectively. We would like to thank F. M. Cornejo-Castillo for valuable insights and discussion on the preliminary results of this manuscript.

Data Availability Statement

All the data generated by this experiment and supporting results and figures are available in the Figshare repository at figshare/b45dd99d490237ff23d1. *nifH* and 16S amplicon sequencing data are

deposited in NCBI BioSample database and are accessible through the BioProject accession number PRJNA1099264 (https://www.ncbi.nlm.nih.gov/sra/PRJNA1099264). Additional Supporting Information can be found in the online version of this article. The results of the GNPS molecular networking with metabolite identification can be found for C18 analysis at: https://gnps.ucsd.edu/ProteoSAFe/status.jsp?task=b3e0015f19c544c1a155ee99415d6d2c and for the ZIC-HILIC analysis at: https://gnps.ucsd.edu/ProteoSAFe/status.jsp?task=32e8c60be66b4bf9a690f611c7d52cb6. The LCMS raw spectra (.mzXML, .RAW), samples list and the compounds lists have been deposited in the MassIVE metabolomics repository (C18 dataset MassIVE MSV000096448: ftp://MSV000096448@massive.ucsd.edu ; Zic-Hilic Dataset MassIVE MSV000096449: ftp://MSV000096449@massive.ucsd.edu).

Funding Statement

This research was supported by the BNP Paribas Foundation for Climate and Biodiversity project NOTION (MB) and the NSF grant OCE-2023498 (KT-K), and also benefited from the ASIA platform (Université de Lorraine-INRAE; https://a2f.univ-lorraine.fr/en/asia-2/). MB was partly funded by the BIOPOLE National Capability Multicentre Round 2 funding from the Natural Environment Research Council (grant no. NE/W004933/1). The MIMS equipment used in this study was obtained with European FEDER Funds. M. Vallet acknowledges the Deutsche Forschungsgemeinschaft (DFG, German Research Foundation), Friedrich Schiller Universität Jena, and is supported by the consortium SFB1127 ChemBioSys, Project number 239748522.

Competing Interests

The authors declare no competing interests.

References

1. Fu F xue, Yu E, Garcia NS, Gale J, Luo Y, Webb EA, et al. Differing responses of marine N_2 fixers to warming and consequences for future diazotroph community structure. 2014;72:33–46. https://doi.org/10.3354/ame01683
2. Yamaguchi T, Sato M, Gonda N, Takahashi K, Furuya K. Phosphate diester utilization by marine diazotrophs Trichodesmium erythraeum and Crocosphaera watsonii. *Aquatic Microbial Ecology* 2020;85:211–218.
3. Thompson AW, Foster RA, Krupke A, Carter BJ, Musat N, Vaulot D, et al. Unicellular cyanobacterium symbiotic with a single-celled eukaryotic alga. *Science (1979)* 2012;337:1546–1550.
4. Coale TH, Loconte V, Turk-Kubo KA, Vanslembrouck B, Mak WKE, Cheung S, et al. Nitrogen-fixing organelle in a marine alga. *Science (1979)* 2024;384:217–222.
5. Farnelid H, Andersson AF, Bertilsson S, Al-Soud WA, Hansen LH, Sørensen S, et al. Nitrogenase gene amplicons from global marine surface waters are dominated by genes of non-cyanobacteria. *PLoS One* 2011;6:e19223.
6. Riemann L, Farnelid H, Steward GF. Nitrogenase genes in non-cyanobacterial plankton: prevalence, diversity and regulation in marine waters. *Aquatic Microbial Ecology* 2010;61:235–247.
7. Turk-Kubo KA, Gradoville MR, Cheung S, Cornejo-Castillo FM, Harding KJ, Morando M, et al. Non-cyanobacterial diazotrophs: Global diversity, distribution, ecophysiology, and activity in marine waters. *FEMS Microbiol Rev* 2022.
8. Acinas SG, Sánchez P, Salazar G, Cornejo-Castillo FM, Sebastián M, Logares R, et al. Deep ocean metagenomes provide insight into the metabolic architecture of bathypelagic microbial communities. *Commun Biol* 2021;4:604.
9. Bentzon-Tilia M, Severin I, Hansen LH, Riemann L. Genomics and ecophysiology of heterotrophic nitrogen-fixing bacteria isolated from estuarine surface water. *mBio* 2015;6:10–1128.

10. Harding KJ, Turk-Kubo KA, Mak EWK, Weber PK, Mayali X, Zehr JP. Cell-specific measurements show nitrogen fixation by particle-attached putative non-cyanobacterial diazotrophs in the North Pacific Subtropical Gyre. *Nat Commun* 2022;13:6979.

11. Fernández-Juárez V, Hallstrøm S, Pacherres CO, Wang J, Coll-Garcia G, Kühl M, et al. Biofilm formation and cell plasticity drive diazotrophy in an anoxygenic phototrophic bacterium. *Appl Environ Microbiol* 2023;89:e01027-23.

12. Bombar D, Paerl RW, Riemann L. Marine non-cyanobacterial diazotrophs: moving beyond molecular detection. *Trends Microbiol* 2016;24:916–927.

13. Moisander PH, Zhang R, Boyle EA, Hewson I, Montoya JP, Zehr JP. Analogous nutrient limitations in unicellular diazotrophs and Prochlorococcus in the South Pacific Ocean. *ISME J* 2012;6:733–744.

14. Rahav E, Giannetto MJ, Bar-Zeev E. Contribution of mono and polysaccharides to heterotrophic N_2 fixation at the eastern Mediterranean coastline. *Sci Rep* 2016;6:27858.

15. Benavides M, Berthelot H, Duhamel S, Raimbault P, Bonnet S. Dissolved organic matter uptake by Trichodesmium in the Southwest Pacific. *Nature Publishing Group* 2017;3–8. https://doi.org/10.1038/srep41315

16. Benavides M, Martias C, Elifantz H, Berman-Frank I, Dupouy C, Bonnet S. Dissolved organic matter influences N_2 fixation in the New Caledonian lagoon (Western Tropical South Pacific). *Front Mar Sci* 2018;5:89.

17. Benavides M, Duhamel S, Van Wambeke F, Shoemaker KM, Moisander PH, Salamon E, et al. Dissolved organic matter stimulates N_2 fixation and nifH gene expression in Trichodesmium. *FEMS Microbiol Lett* 2020;367:fnaa034.

18. Bonnet S, Dekaezemacker J, Turk-Kubo KA, Moutin T, Hamersley RM, Grosso O, et al. Aphotic N_2 fixation in the eastern tropical South Pacific Ocean. *PLoS One* 2013;8:e81265.

19. Rahav E, Bar-Zeev E, Ohayon S, Elifantz H, Belkin N, Herut B, et al. Dinitrogen fixation in aphotic oxygenated marine environments. *Front Microbiol* 2013;4:227.

20. Hutchins DA, Capone DG. The marine nitrogen cycle: New developments and global change. *Nat Rev Microbiol* 2022;20:401–414.

21. Filella A, Umbricht J, Klett A, Vogts A, Vannier T, Grosso O, et al. Dissolved organic matter offsets the detrimental effects of climate change in the nitrogen-fixing cyanobacterium Crocosphaera. *Limnol Oceanogr Lett* 2024;9:296–306.

22. Moran MA, Kujawinski EB, Stubbins A, Fatland R, Aluwihare LI, Buchan A, et al. Deciphering ocean carbon in a changing world. *Proc Natl Acad Sci U S A* 2016;113:3143–3151. https://doi.org/10.1073/pnas.1514645113

23. Kieft B, Li Z, Bryson S, Hettich RL, Pan C, Mayali X, et al. Phytoplankton exudates and lysates support distinct microbial consortia with specialized metabolic and ecophysiological traits. *Proceedings of the national academy of sciences* 2021;118:e2101178118.

24. Kujawinski EB. The impact of microbial metabolism on marine dissolved organic matter. *Ann Rev Mar Sci* 2011;3:567–599.

25. Hansell DA. Recalcitrant dissolved organic carbon fractions. *Ann Rev Mar Sci* 2013;5:421–445.

26. Mopper K, Stubbins A, Ritchie JD, Bialk HM, Hatcher PG. Advanced instrumental approaches for characterization of marine dissolved organic matter: extraction techniques, mass spectrometry, and nuclear magnetic resonance spectroscopy. *Chem Rev* 2007;107:419–442.

27. Zark M, Christoffers J, Dittmar T. Molecular properties of deep-sea dissolved organic matter are predictable by the central limit theorem: Evidence from tandem FT-ICR-MS. *Mar Chem* 2017;191:9–15.

28. Dittmar T, Lennartz ST, Buck-Wiese H, Hansell DA, Santinelli C, Vanni C, et al. Enigmatic persistence of dissolved organic matter in the ocean. *Nat Rev Earth Environ* 2021;2:570–583.

29. Hertkorn N, Ruecker C, Meringer M, Gugisch R, Frommberger M, Perdue EM, et al. High-precision frequency measurements: indispensable tools at the core of the molecular-level analysis of complex systems. Anal Bioanal Chem. 2007;389:1311–27.

30. Riedel T, Dittmar T. A method detection limit for the analysis of natural organic matter via Fourier transform ion cyclotron resonance mass spectrometry. Anal Chem. 2014;86(16):8376–82.

31. Neufeld JD, Vohra J, Dumont MG, Lueders T, Manefield M, Friedrich MW, et al. DNA stable-isotope probing. Nat Protoc. 2007;2(4):860–6.

32. Carlson CA, Giovannoni SJ, Hansell DA, Goldberg SJ, Parsons R, Otero MP, et al. Effect of nutrient amendments on bacterioplankton production, community structure, and DOC utilization in the northwestern Sargasso Sea. Aquatic microbial ecology. 2002;30(1):19–36.

33. Carlson CA, Giovannoni SJ, Hansell DA, Goldberg SJ, Parsons R, Vergin K. Interactions among dissolved organic carbon, microbial processes, and community structure in the mesopelagic zone of the northwestern Sargasso Sea. Limnol Oceanogr. 2004;49(4):1073–83.

34. Xia J, Psychogios N, Young N, Wishart DS. MetaboAnalyst: a web server for metabolomic data analysis and interpretation. Nucleic Acids Res. 2009;37(suppl_2):W652–60.

35. Dumont MG, Murrell JC. Stable isotope probing—linking microbial identity to function. Nat Rev Microbiol. 2005;3(6):499–504.

36. Radajewski S, Ineson P, Parekh NR, Murrell JC. Stable-isotope probing as a tool in microbial ecology. Nature. 2000;403(6770):646–9.

37. Felske A, Akkermans ADL, De Vos WM. Quantification of 16S rRNAs in complex bacterial communities by multiple competitive reverse transcription-PCR in temperature gradient gel electrophoresis fingerprints. Appl Environ Microbiol. 1998;64(11):4581–7.

38. Cébron A, Norini MP, Beguiristain T, Leyval C. Real-Time PCR quantification of PAH-ring hydroxylating dioxygenase (PAH-RHDα) genes from Gram positive and Gram negative bacteria in soil and sediment samples. J Microbiol Methods. 2008;73(2):148–59.

39. Huguet A, Vacher L, Relexans S, Saubusse S, Froidefond JM, Parlanti E. Properties of fluorescent dissolved organic matter in the Gironde Estuary. Org Geochem. 2009;40(6):706–19.

40. Catalá TS, Reche I, Fuentes-Lema A, Romera-Castillo C, Nieto-Cid M, Ortega-Retuerta E, et al. Turnover time of fluorescent dissolved organic matter in the dark global ocean. Nat Commun. 2015;6.

41. Helms JR, Stubbins A, Perdue EM, Green NW, Chen H, Mopper K. Photochemical bleaching of oceanic dissolved organic matter and its effect on absorption spectral slope and fluorescence. Mar Chem. 2013;155:81–91.

42. Berthelot H, Duhamel S, L'Helguen S, Maguer JF, Wang S, Cetinić I, et al. NanoSIMS single cell analyses reveal the contrasting nitrogen sources for small phytoplankton. ISME Journal. 2019;13(3):651–62.

43. Selden CR, Chappell PD, Clayton S, Macías-Tapia A, Bernhardt PW, Mulholland MR. A coastal N_2 fixation hotspot at the Cape Hatteras front: elucidating spatial heterogeneity in diazotroph activity via supervised machine learning. Limnol Oceanogr. 2021;66(5):1832–49.

44. Moisander PH, Serros T, Paerl RW, Beinart RA, Zehr JP. Gammaproteobacterial diazotrophs and nifH gene expression in surface waters of the South Pacific Ocean. ISME J. 2014;8(10):1962–73.

45. Langlois R, Großkopf T, Mills M, Takeda S, LaRoche J. Widespread distribution and expression of gamma A (UMB), an uncultured, diazotrophic, γ-proteobacterial nifH phylotype. PLoS One. 2015;10(6):e0128912.

46. Halm H, Lam P, Ferdelman TG, Lavik G, Dittmar T, Laroche J, et al. Heterotrophic organisms dominate nitrogen fixation in the south pacific gyre. ISME Journal. 2011;6(6):1238–49.

47. Loescher CR, Großkopf T, Desai FD, Gill D, Schunck H, Croot PL, et al. Facets of diazotrophy in the oxygen minimum zone waters off Peru. ISME J. 2014;8(11):2180–92.

48. Wu C, Narale DD, Cui Z, Wang X, Liu H, Xu W, et al. Diversity, structure, and distribution of bacterioplankton and diazotroph communities in the Bay of Bengal during the winter monsoon. Front Microbiol. 2022;13:987462.

49. Martínez-Pérez C, Mohr W, Schwedt A, Dürschlag J, Callbeck CM, Schunck H, et al. Metabolic versatility of a novel N_2-fixing Alphaproteobacterium isolated from a marine oxygen minimum zone. Environ Microbiol. 2018;20(2):755–68.

50. Wu C, Sun J, Liu H, Xu W, Zhang G, Lu H, et al. Evidence of the significant contribution of heterotrophic diazotrophs to nitrogen fixation in the Eastern Indian Ocean during pre-southwest monsoon period. Ecosystems. 2021;1–18.

51. Howat AM, Vollmers J, Taubert M, Grob C, Dixon JL, Todd JD, et al. Comparative genomics and mutational analysis reveals a novel XoxF-utilizing methylotroph in the Roseobacter group isolated from the marine environment. Front Microbiol. 2018;9:766.

52. Delmont TO, Pierella Karlusich JJ, Veseli I, Fuessel J, Eren AM, Foster RA, et al. Heterotrophic bacterial diazotrophs are more abundant than their cyanobacterial counterparts in metagenomes covering most of the sunlit ocean. ISME J. 2022;16(4):927–36.

53. Durán-Viseras A, Castro DJ, Reina JC, Béjar V, Martínez-Checa F. Taxogenomic and metabolic insights into Marinobacterium ramblicola sp. nov., a new slightly halophilic bacterium isolated from Rambla Salada, Murcia. Microorganisms. 2021;9(8):1654.

54. Yoch DC. Dimethylsulfoniopropionate: its sources, role in the marine food web, and biological degradation to dimethylsulfide. Appl Environ Microbiol. 2002;68(12):5804–15.

55. Boden R, Murrell JC, Schäfer H. Dimethylsulfide is an energy source for the heterotrophic marine bacterium Sagittula stellata. FEMS Microbiol Lett. 2011;322(2):188–93.

56. Meyer N, Rydzyk A, Pohnert G. Pronounced uptake and metabolism of organic substrates by diatoms revealed by pulse-labeling metabolomics. Front Mar Sci. 2022;9:821167.

57. Gebser B, Pohnert G. Synchronized regulation of different zwitterionic metabolites in the osmoadaption of phytoplankton. Mar Drugs. 2013;11(6):2168–82.

58. Wang J, Yao H. Applications of DNA/RNA-stable isotope probing (SIP) in environmental microbiology. In: Methods in Microbiology. Elsevier; 2021. p. 227–67.

59. Turk-Kubo KA, Gradoville MR, Cheung S, Cornejo-Castillo FM, Harding KJ, Morando M, et al. Non-cyanobacterial diazotrophs: global diversity, distribution, ecophysiology, and activity in marine waters. FEMS Microbiol Rev. 2023;47(6):fuac046.

60. Strom SL, Benner R, Ziegler S, Dagg MJ. Planktonic grazers are a potentially important source of marine dissolved organic carbon. Limnol Oceanogr. 1997;42(6):1364–74.

61. Jumars PA, Penry DL, Baross JA, Perry MJ, Frost BW. Closing the microbial loop: dissolved carbon pathway to heterotrophic bacteria from incomplete ingestion, digestion and absorption in animals. Deep Sea Research Part A Oceanographic Research Papers. 1989;36(4):483–95.

62. Mills MM, Turk-Kubo KA, van Dijken GL, Henke BA, Harding K, Wilson ST, et al. Unusual marine cyanobacteria/haptophyte symbiosis relies on N_2 fixation even in N-rich environments. ISME Journal [Internet]. 2020;14(10):2395–406. Available from: http://dx.doi.org/10.1038/s41396-020-0691-6

63. Cornejo-Castillo FM, Inomura K, Zehr JP, Follows MJ. Metabolic trade-offs constrain the cell size ratio in a nitrogen-fixing symbiosis. Cell. 2024;187(7):1762–8.

64. Mak EWK, Turk-Kubo KA, Caron DA, Harbeitner RC, Magasin JD, Coale TH, et al. Phagotrophy in the nitrogen-fixing haptophyte Braarudosphaera bigelowii. Environ Microbiol Rep. 2024;16(4):e13312.

65. Tripp HJ, Bench SR, Turk KA, Foster RA, Desany BA, Niazi F, et al. Metabolic streamlining in an open-ocean nitrogen-fixing cyanobacterium. Nature. 2010;464(7285):90–4.

66. Agawin NSR, Benavides M, Busquets A, Ferriol P, Stal LJ, Arístegui J. Dominance of unicellular cyanobacteria in the diazotrophic community in the Atlantic Ocean. Limnol Oceanogr. 2014;59(2):623–37.

67. Harding K, Turk-kubo KA, Sipler RE, Mills MM, Bronk DA. Symbiotic unicellular cyanobacteria fix nitrogen in the Arctic Ocean. 2018;115(52).

68. Turk-Kubo KA, Mills MM, Arrigo KR, van Dijken G, Henke BA, Stewart B, et al. UCYN-A/haptophyte symbioses dominate N_2 fixation in the Southern California Current System. ISME communications. 2021;1(1):42.

69. Landa M, Turk-Kubo KA, Cornejo-Castillo FM, Henke BA, Zehr JP. Critical role of light in the growth and activity of the marine N_2-fixing UCYN-A symbiosis. Front Microbiol. 2021;12:666739.

70. Wirth JS, Wang T, Huang Q, White RH, Whitman WB. Dimethylsulfoniopropionate sulfur and methyl carbon assimilation in Ruegeria species. mBio. 2020;11(2):10–1128.

71. Reeder CF, Filella A, Voznyuk A, Coët A, James RC, Rohrer T, et al. Unveiling the contribution of particle-associated non-cyanobacterial diazotrophs to N_2 fixation in the upper mesopelagic North Pacific Gyre. Commun Biol. 2025;8(1):287.

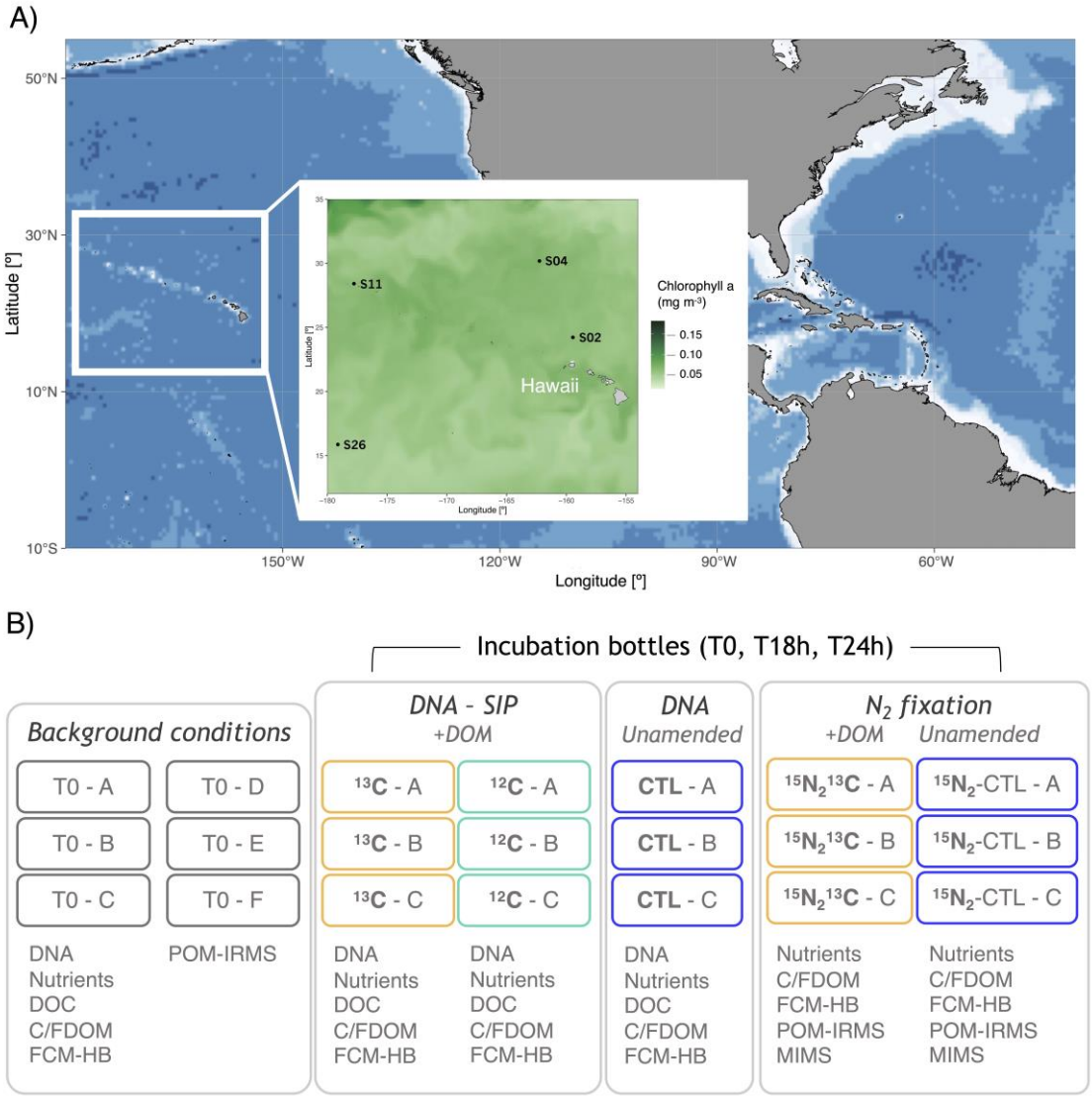

Fig. 1. Surface (10m) Chlorophyll-*a* station map (A) and experimental design showing incubations performed onboard (B). Stations are superimposed on sea surface Chlorophyll-*a* concentration (mg m^{-3}) obtained from 1/4º 10 day-binned COPERNICUS satellite data (https://data.marine.copernicus.eu/viewer) from 1 June to 1 July 2022. 'T0' stands for time zero, '^{13}C' and '^{12}C' treatments indicate that the bottles were enriched with phytoplankton-derived labeled DOM previously produced in the lab (+DOM), 'CTL' represents control incubations without added DOM and '$^{15}N_2$' shows the bottles that received enriched filtered seawater for N_2 fixation measurements. Letters A-F refer to experimental replicates. DNA from incubations was used for *nifH* and *16S-rRNA* datasets.

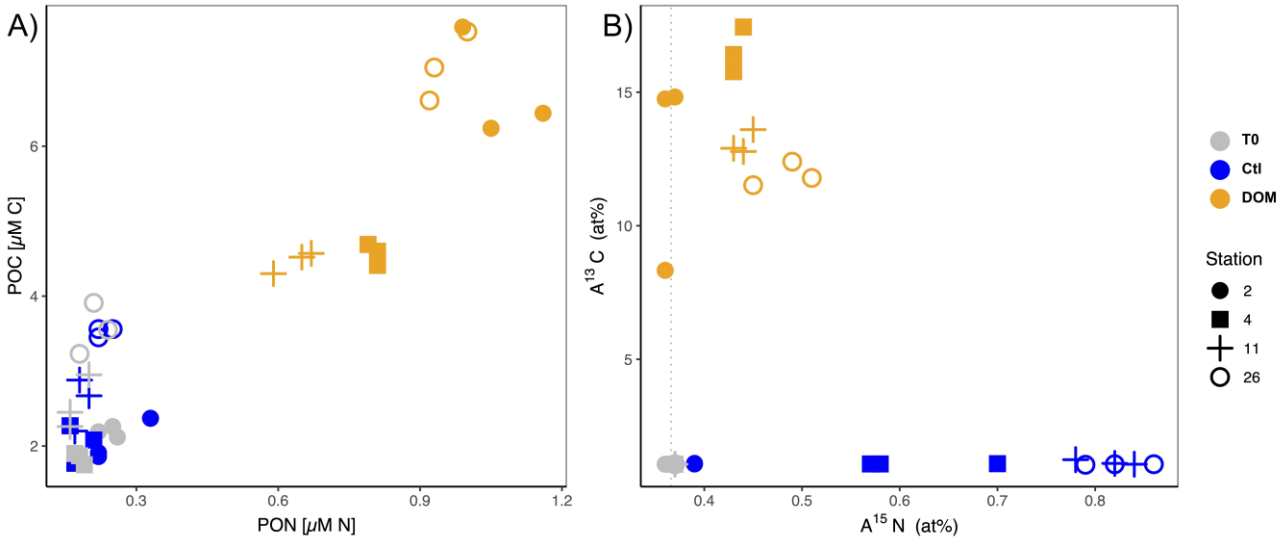

Fig. 2. Bulk particulate organic matter (POC and PON; µM) (A) and atom ^{15}N and ^{13}C enrichments (at%) (B) from initial background samples (T0; grey), and after 24 h incubation of unamended (Ctl T24: Control; blue) and DOM-amended samples (DOM T24; orange) for each station (2, 4, 11 and 26; depicted by different shape).

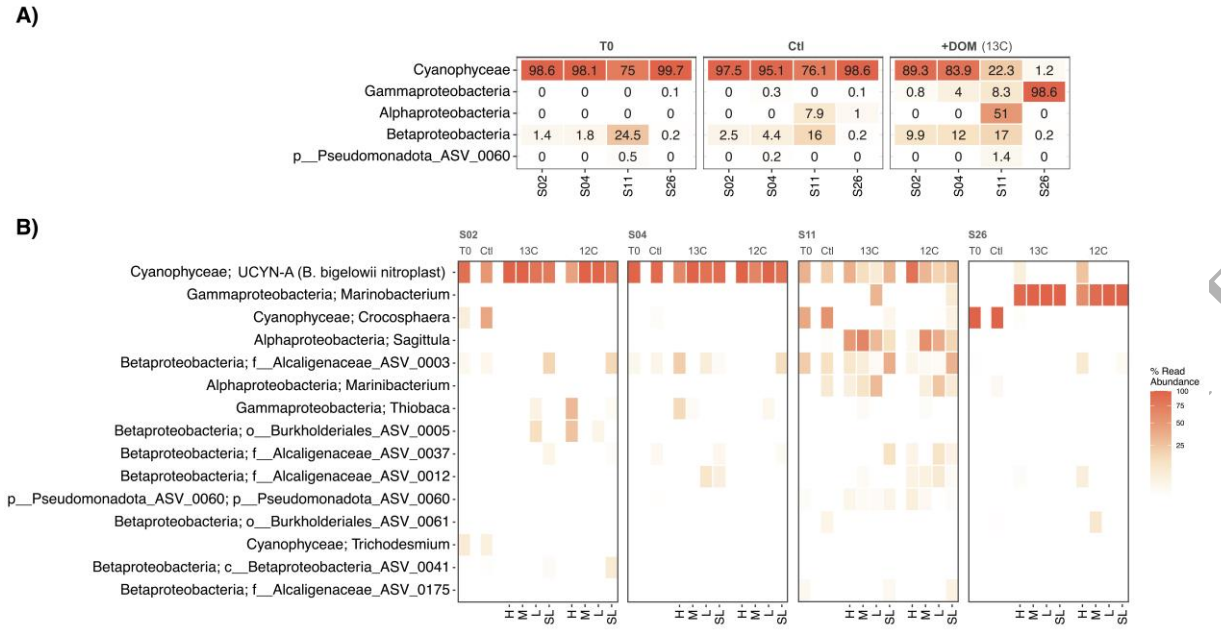

Fig. 3. Heatmap showing the relative abundance of *nifH* gene reads in the diazotroph community for 'T0' and post-incubation samples (unamended or 'Ctl' and amended with either ^{13}C- or ^{12}C-DOM) at each station. The relative abundance of *nifH* reads is sorted by the most abundant class (A), and the top 15 most abundant taxa are further divided by genus (B) and into the different DNA density fractions (heavy 'H', medium 'M', light L' and superlight 'SL').

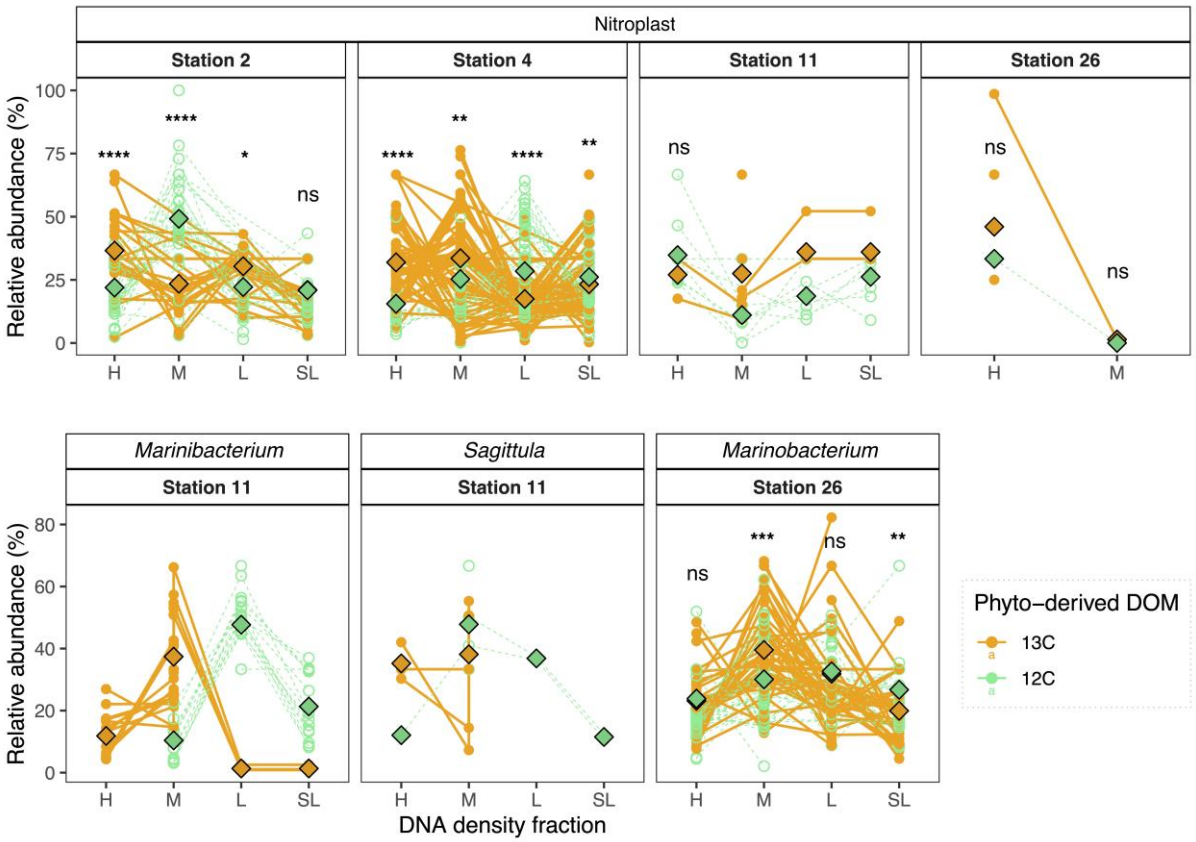

Fig. 4. *nifH* gene relative abundance of enriched (higher in ^{13}C fractions) amplicon sequence variant (ASVs) (assigned to Genus) across DOM treatments (^{13}C-labeled: filled dot and solid line, and ^{12}C-labeled; open dot and dashed line) and density fractions (heavy or 'H', medium or 'M', light or 'L' and super-light or 'SL'). Each point represents the average of the three experimental replicates. Different lines within each panel indicate different ASVs assigned to the same genus. Diamond dots show the average of all ASVs in each fraction and treatment. Significant differences in relative abundance between DOM treatments were tested with the Kruskal-Wallis Test and shown as significant codes (****; $p < 0.0001$, ***; $p < 0.001$, **; $p < 0.01$, *; $p < 0.1$, ns; not significant).

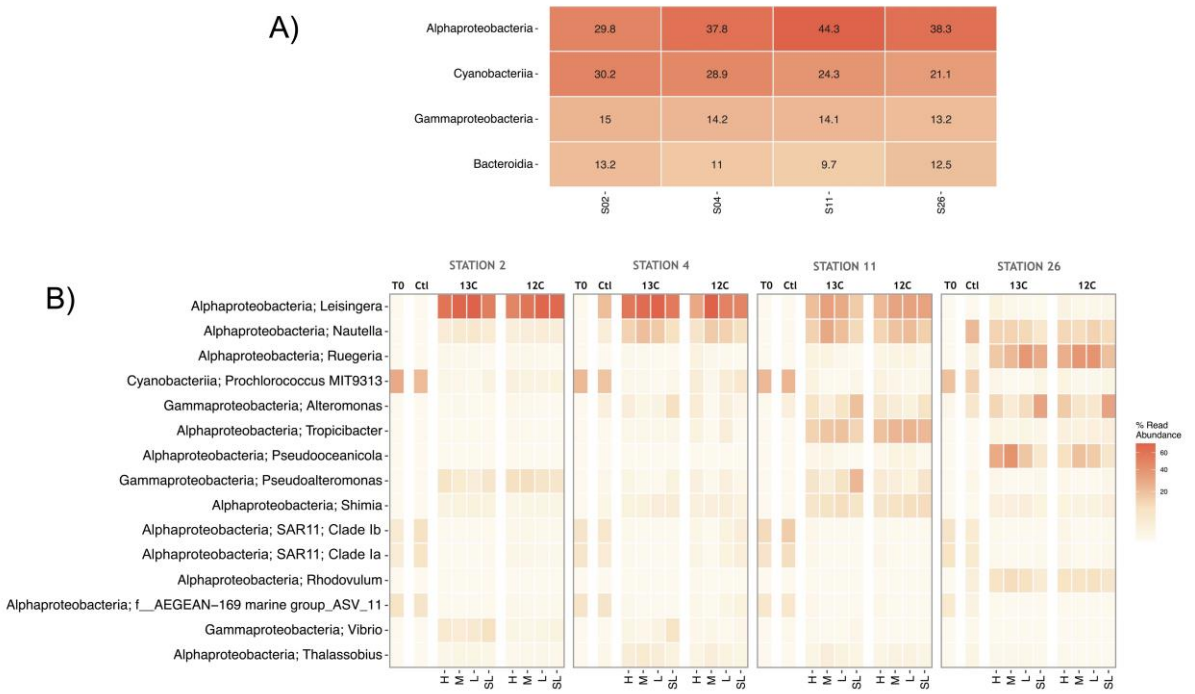

Fig. 5. Heatmap showing the relative abundance of 16S rRNA gene amplicon reads assigned to the four most abundant classes at 'T0' (A) and to the 15 most abundant ASVs shared between 'T0' and post-incubation samples (unamended or 'Ctl' and amended with ^{13}C- or ^{12}C-DOM) (B) for each station. For each taxon shown in B, the relative abundance of 16S rRNA gene reads is further divided into the different DNA density fractions (heavy or 'H', medium or 'M', light or 'L' and superlight or 'SL').

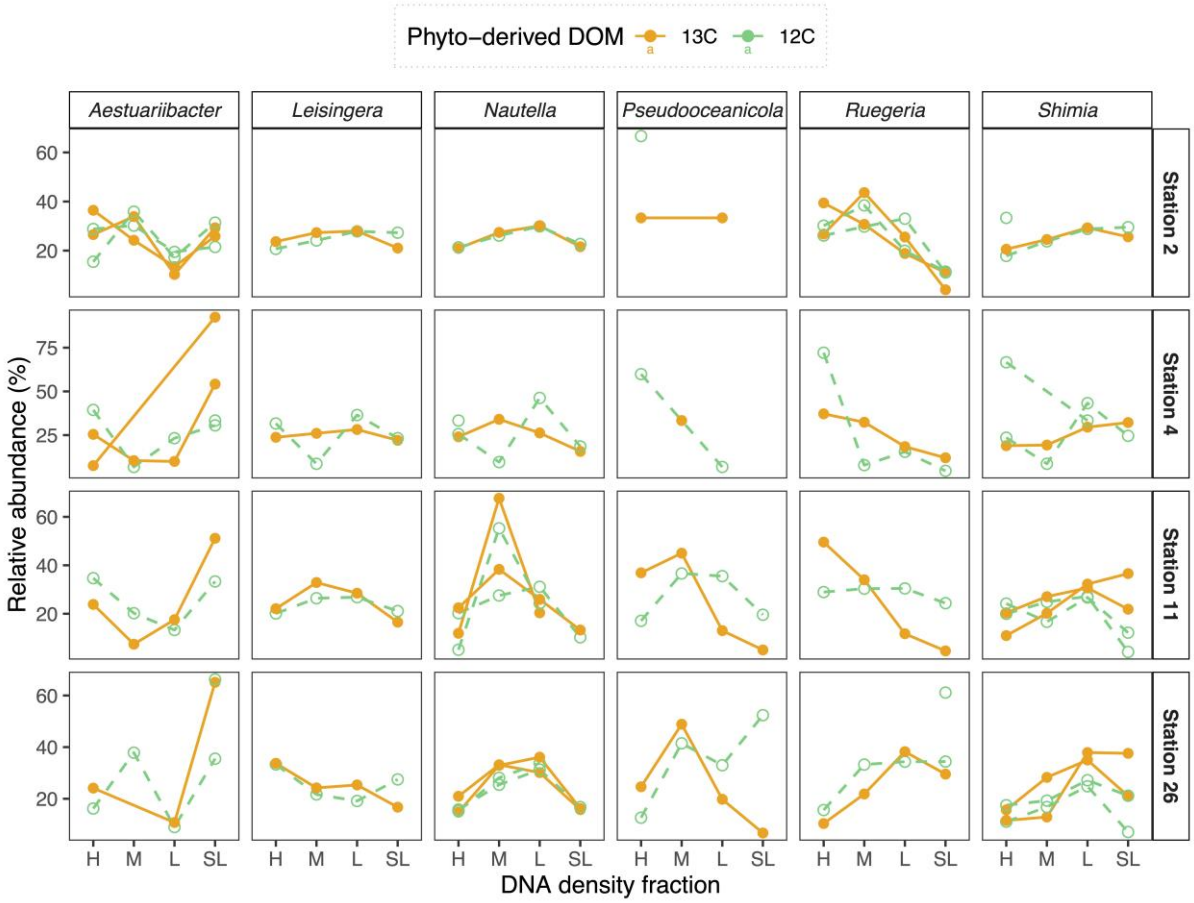

Fig. 6. Relative abundance (16S rRNA gene) profiles of enriched (higher in ^{13}C fractions) ASVs (assigned to Genus) across DOM treatments (^{13}C-labeled: filled dot and solid line, and ^{12}C-unlabelled; open dot and dashed line) and density fractions (heavy or 'H', medium or 'M', light or 'L' and super-light or 'SL'). Each point represents the average of the three experimental replicates. Different lines within each panel indicate different ASVs assigned to the same genus.

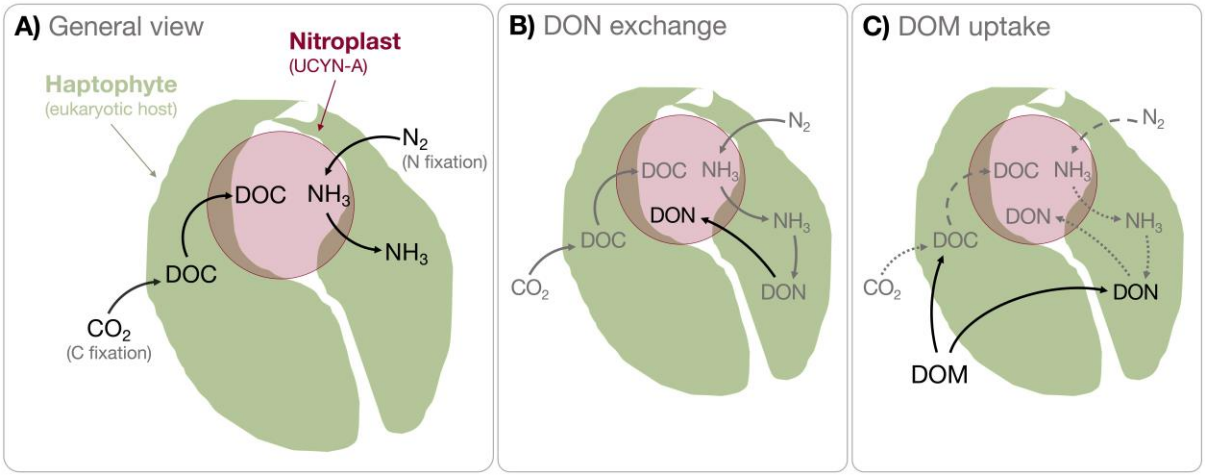

Fig. 7. Schematic figure illustrating the known (A, B) and potential (C) carbon and nitrogen acquisition and exchange pathways between the environment and the haptophyte *Braarudosphaera bigelowii* and its nitroplast. Dotted lines indicate when the process might be decreased due to a new type of uptake or reallocation of resources.